

Radiative charge transfer in $\text{Ne}^{2+} + \text{He}$ collisions

L. B. Zhao¹, J. G. Wang², P. C. Stancil¹, J. P. Gu³,
H.-P. Liebermann³, R. J. Buenker³, and M. Kimura⁴

¹*Department of Physics and Astronomy and Center for Simulational Physics,
University of Georgia, Athens, GA 30602-2451, USA*

²*Institute of Applied Physics and Computational Mathematics,
Beijing 100088, People's Republic of China*

³*Fachbereich C-Mathematik und Naturwissenschaften,
Bergische Universität Wuppertal, D-42097 Wuppertal, Germany and*

⁴*Graduate School of Sciences, Kyushu University, Fukuoka 812-8581, Japan*

(Dated: August 10, 2006)

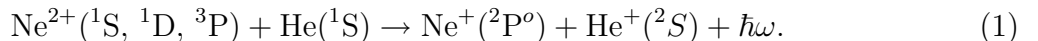
Abstract

The optical potential and semiclassical methods have been applied to studies of radiative charge transfer in collisions of ground-state and metastable Ne^{2+} ions with neutral helium. Cross sections are presented with relative collision energies between 0.1 meV and 10 keV. For all transitions concerned, the cross sections display rich resonance structures in the low-energy region. From the calculated cross sections, rate coefficients are obtained with temperatures between 10 and 20×10^6 K and found to be in agreement with available experiment data. The multireference single- and double-excitation configuration-interaction (MRD-CI) method was used to obtain the relevant adiabatic molecular potentials and dipole transition matrix elements.

I. INTRODUCTION

Ne^{2+} and Ne^+ ions are abundant in low-temperature or ultracold plasmas, such as produced in magneto-optical traps and found in interstellar space. The populations of Ne^{2+} and Ne^+ ions and their emission spectra may be significantly influenced by direct or radiative charge transfer due to collisions of neon ions and neutral helium. A number of studies have been made to understand these dynamical processes (see, e.g., [1–3]). The efforts focused mainly on measurements and calculations of direct charge transfer in the energy region from a few eV to keV where direct charge transfer dominates. However, for many charge transfer systems, cross sections for direct charge transfer rapidly decrease with decreasing energy below a few eV [4, 5] and radiative charge transfer becomes dominant in the sub-eV energy region. Many investigations have substantiated such a conclusion (see, e.g., [5–7]). In order to simulate cold or ultracold plasmas with neon ions and neutral helium, it is necessary to provide accurate cross sections for radiative charge transfer in collisions of neon ions and neutral helium. However, to the best of our knowledge, there exists only one measurement for radiative charge transfer in collisions of Ne^{2+} with He at 300 K [8], while no theoretical studies have been performed.

In this paper, we report investigations of radiative charge transfer in collisions of ground-state and metastable Ne^{2+} with He. The optical potential and semiclassical methods are used to calculate the cross sections. The concerned processes include the radiative charge transfer reactions



The relevant adiabatic molecular potentials and dipole transition matrix elements were obtained with the multireference single- and double-excitation configuration-interaction (MRD-CI) method [9–12].

II. MOLECULAR STRUCTURE CALCULATIONS

The adiabatic potential energies and molecular electronic wave functions of the NeHe^{2+} system were obtained with the MRD-CI method [9–11] with configuration selection at a threshold of 1.0×10^{-7} a.u. and energy extrapolation using the TABLE CI algorithm [12]. The two electrons in the lowest molecular orbital were kept inactive in the present CI

calculation and the highest molecular orbital was discarded. In the calculation of neon ions, the cc-pVQZ correlation-consistent, polarization valence, quadruple- ζ basis set is used [13], but the g function in this basis set is discarded. In addition to the above basis set, several diffuse functions are added. The basis set for the neon atoms is thus $(14s8p3d2f)$, contracted to $[7s6p3d2f]$. For the helium atom, the $(7s3p)/[5s3p]$ basis set of Roemelt *et al* [14] was employed and one d -type function with an exponent of 1.0 was added. The parameters used in the present MRD-CI calculations are given by Imai *et al* [3]. The potentials and dipole transition matrix elements were calculated from the internuclear distance $R = 1.6$ to $20.0 a_0$.

The ten adiabatic potential curves are plotted as a function of the internuclear distance R in figure 1. The four electronic states $1^1\Sigma^+$, $1^1\Pi$, $1^3\Sigma^+$ and $1^3\Pi$ are formed in the approach of $\text{Ne}^+(^2P^o)$ with He^+ , the two states $1^3\Sigma^-$ and $2^3\Pi$ by $\text{Ne}^{2+}(^3P)$ with He , the two states $1^1\Delta$, $2^1\Pi$ and $2^1\Sigma^+$ by $\text{Ne}^{2+}(^1D)$ with He , and the state $3^1\Sigma^+$ by $\text{Ne}^{2+}(^1S)$ with He . The calculated MRD-CI asymptotic energies are presented for the ten molecular states relative to the $\text{Ne}^{2+}(^3P) + \text{He}$ channel and compared with available theoretical and experimental energies in table 1. Good agreement is seen with not only available theoretical results and also measurements. The maximum relative errors of the current results from the experimental data is less than 2%.

Beyond $R = 20.0$ a.u., the potentials for the entrance channels are described by the charge-induced-dipole interactions

$$V_L(R) = -\frac{\alpha_d}{2R^4} + E_\infty, \quad (2)$$

where α_d is the dipole polarizability of the neutral He atom and E_∞ is the separated-atom energy. All the quantities in Eq. (2) are in atomic units (a.u.). For the exit channels, the long-range potentials ($R > 20.0$ a.u.) are coulombic. E_∞ is determined using these parameters and the *ab initio* potentials.

The ten dipole transition matrix elements $D(R)$ from the six initial molecular states to the four final states are presented as a function of R in figures 2(a) and 2(b). From the figures, one can find that the matrix elements are larger for transitions between molecular states of the same symmetries than for transitions between states of different symmetries. In table 2, the MRD-CI dipole transition matrix elements at $R = 2.5$ and $8.0 a_0$ are compared with those of Mercier *et al* [15] and Ben-Itzhak *et al* [16]. For the strong transitions, agreement

is satisfactory between our results and those of Mercier *et al* and Ben-Itzhak *et al*, while for the weaker transitions, such as $2\ ^1\Pi \rightarrow 1\ ^1\Sigma^+$ and $1\ ^3\Sigma^- \rightarrow 1\ ^3\Pi$, there are larger differences. However, this is not astonishing. For any theory, it is a thorny task to obtain physical quantities of relatively good precision for weak transitions. Furthermore, it should be mentioned that the long-range asymptotic behavior of $D(R)$ is fitted to the form $\frac{d_0}{R^n}$.

III. THEORY FOR RADIATIVE CHARGE TRANSFER

An optical potential method to treat radiative decay induced by ion-atom collisions has been described in detail by Zygelman and Dalgarno [17] and successfully applied to calculations of some systems [6, 7]. Here we only outline the method and relevant formulae. During ion-atom collisions, a particle flux may be lost due to radiative emission. It is assumed that the transition probability per unit time from a high-lying molecular state to a low-lying molecular state is represented by the imaginary part of a complex optical potential. The amplitude $F_a(\mathbf{R})$ is the solution of the Schrödinger equation,

$$\left[-\frac{1}{2\mu}\nabla_{\mathbf{R}}^2 + \frac{1}{2\mu R^2}\Lambda^2 + V_a(R) - E \right] F_a(\mathbf{R}) = \frac{i}{2}A(R)F_a(\mathbf{R}) \quad (3)$$

where μ is the reduced mass of the ion-atom pair, Λ is the orbital angular momentum projection quantum number, $V_a(R)$ is the adiabatic potential energy for the high-lying molecular state a , E is the relative collision energy in the center-of-mass frame, and $A(R)$ is the probability per unit time for the radiative transition given by

$$A(R) = \frac{4}{3}D^2(R)\frac{|V_b(R) - V_a(R)|^3}{c^3} \quad (4)$$

where c is the speed of light and $V_b(R)$ is the adiabatic potential energy for the low-lying molecular state b . The cross section for collision-induced radiative decay, including radiative charge transfer and radiative association, can be written as

$$\sigma(E) = \frac{\pi}{k_a^2} \sum_J^{\infty} (2J+1)[1 - \exp(-4\eta_J)] \quad (5)$$

where η_J is the imaginary part of the phase shift of the J th partial wave of the radial Schrödinger equation which is given in the distorted-wave approximation by

$$\eta_J = \frac{\pi}{2} \int_0^{\infty} dR |f_J^a(k_a R)|^2 A(R) \quad (6)$$

and $f_j^g(R)$ is the regular solution of the partial-wave Schrödinger equation, obtained from equation (3) by introducing a partial-wave decomposition for the amplitude $F_a(\mathbf{R})$. It should be pointed that, in general, contributions from radiative association to collision-induced radiative decay are very small and radiative charge transfer dominates radiation association for the considered collision energies. In this particular system, radiative association may only proceed through transitions to the $1^1\Sigma^+$ state which has a very shallow well (~ 0.136 eV) at a short range. Any states formed will be quasi-bound and likely predissociate rapidly [16]. We therefore assume that radiative association is negligible and all radiative decay contributes to charge transfer.

Replacing the summation in equation (5) and applying the JWKB approximation, one obtains the expression for the semiclassical cross section

$$\sigma(E) = 2\pi \sqrt{\frac{2\mu}{E}} \int p \, dp \int_{R_a^{\text{ctp}}}^{\infty} dR \frac{A(R)}{\sqrt{1 - V_a(R)/E - p^2/R^2}} \quad (7)$$

where p is the impact parameter and R_a^{ctp} is the classical turning point in the incoming channel [17].

IV. RESULTS AND DISCUSSION

State-to-state cross sections for radiative charge transfer are evaluated using the adiabatic potentials and dipole matrix elements in section 2. The contributions from the individual partial waves are summed as in equation (5) until a convergence of the cross sections is achieved. The results for all ten transitions obtained with the optical potential method are shown as a function of relative collision energy in figures 3(a) and 3(b). The relative collision energy ranges from 0.1 meV to 1 eV. The cross sections for the different transitions vary in magnitude over a wide range. Very rich resonance structures appear in the energy region between 0.1 meV and 0.1 eV. These resonance are attributed to the presence of quasibound or virtual rotational-vibrational levels in the entrance channel, associated with classical orbiting. It is obvious that resonances for transitions with the same initial molecular states should appear in the exact same positions. This phenomenon is readily seen in figures 3(a) and 3(b), for example, $3^1\Sigma^+ \rightarrow 1^1\Sigma^+$ and $3^1\Sigma^+ \rightarrow 1^1\Pi$. The resonances may give rise to an enhancement in the rate coefficients. Stancil *et al* [6] quantitatively analyzed the contribution from the resonances for collisions of Li and H^+ and showed that such a

contribution is as high as 30% compared to the background.

Figure 3 illustrates that the four dominant radiative decay processes, $3\ ^1\Sigma^+ \rightarrow 1\ ^1\Sigma^+$, $2\ ^1\Sigma^+ \rightarrow 1\ ^1\Sigma^+$, $2\ ^1\Pi \rightarrow 1\ ^1\Pi$ and $2\ ^3\Pi \rightarrow 1\ ^3\Pi$, are due to transitions between molecular states of the same symmetries, and the weaker transitions are smaller than the strong ones by two orders of magnitude or more in the concerned energy region except for the transition $2\ ^3\Pi \rightarrow 1\ ^3\Pi$ at $E < \sim 0.6$ meV. For eight of the ten transitions except for the $2\ ^3\Pi \rightarrow 1\ ^3\Pi$ and $2\ ^3\Pi \rightarrow 1\ ^3\Sigma^+$, the background cross section, excluding resonances, decreases monotonically by more than two orders of magnitude as the relative collision energy increases from 0.1 meV to 1 eV.

Semiclassical calculations of the cross sections for radiative decay have been performed based on equation (7). The relative collision energy ranges from 0.1 eV to 10^4 eV for all ten transitions. The cross sections from the ground state 3P and metastable states 1S and 1D of Ne^{2+} into $Ne^+(^2P^o)$ are presented in figure 4. The corresponding optical potential cross sections are also plotted for comparison between 0.1 eV to 1 eV. It should be pointed out that the cross sections in this figure have been multiplied by the probability factor $p_{\Lambda S}$ whose expression can be found in [7]. The semiclassical approximation is believed to be able to give reliable cross sections in the higher energy region. However, it is noted that even at $E = 0.1$ eV, this approximation produces results in excellent agreement with those from the optical potential method. For large energies ($E \gg V_a$), the double integral in equation (7) is nearly energy independent and therefore $\sigma(E)$ varies as $1/\sqrt{E}$. Our numerical results for all the transitions display such behavior for $E \gtrsim 30$ eV, as seen in the figure. Similar behavior has been seen in collisions of Li and H^+ [6] and O and He^+ [7].

In figure 4, we also compare the current radiative charge transfer cross sections with the direct charge transfer cross sections of Imai *et al* [3] which were obtained with a semiclassical molecular-orbital close-coupling method, but using the same molecular potentials. For $Ne^{2+}(^3P)$, radiative charge transfer dominates for $E < 70$ eV suggesting that it is the most important process in astrophysical environments and ultracold plasmas. On the other hand, the lowest energy point from Imai *et al*'s calculations is at 33.3 eV for the metastable states 1D and 1S where the direct cross sections are two orders of magnitude larger than radiative charge transfer. However, a visual extrapolation of Imai *et al*'s results suggests that radiative charge transfer will become the primary charge transfer mechanism below $\sim 10^{-2}$ eV for the Ne^{2+} metastable states.

Rate coefficients were obtained by averaging the radiative charge transfer cross sections in figure 4 over a Maxwellian velocity distribution and are plotted as a function of temperature T in figure 5. The rate coefficients from $\text{Ne}^{2+}(^1\text{S})$ are much larger than those from the ^1D and ^3P in the concerned temperature region. Each curve has a minimum value near 10^4 K and it rapidly increases with increasing temperature. Above 10^6 K, the rate coefficient for radiative charge transfer display a tendency to approach a constant with increasing T . This is because the cross section behaves as $1/\sqrt{E}$ at large energies. The current rate coefficients are compared to one available experimental value at $T = 300$ K measured by Johnsen and Biondi [8]. As the measurement was unable to separate each ionic state, the measured result is expected to refer to a mixture of all three states. It can be seen that the calculated rate coefficient is in agreement with the measured value if it is assumed that the ionic fraction in the ^1S state is less than 50%. While no previous theoretical study has been performed for radiative charge transfer in this collision system, Dalgarno, Butler and Heil [18] and Butler and Dalgarno [19] argued from examination of the potential energy curves that radiative charge transfer for $\text{Ne}^{2+}(^3\text{P})$ would dominate at low temperatures, but have a rate coefficient no greater than $10^{-14} \text{ cm}^3\text{s}^{-1}$. As seen in figure 5, the current results are consistent with their conclusion, though the computed rate coefficients are a factor of 5-10 smaller.

For convenience, the rate coefficients are fitted to the form

$$\alpha(T) = \sum_i a_i \left(\frac{T}{10,000} \right)^{b_i} \exp \left(-\frac{T}{c_i} \right) \quad (8)$$

where α is the rate coefficient in cm^3/s , T is temperature in K. The fitting parameters are given in table 3. a_i and c_i are in units of $\text{cm}^3 \text{ s}^{-1}$ and K, respectively. The fits do not deviate from the computed rate coefficients by more than 7.8%, 11.3% and 17.5% for radiative decay from ^1S , ^1D and ^3P , respectively.

V. SUMMARY

Cross sections and rate coefficients have been presented for radiative charge transfer due to collisions of ground-state and metastable Ne^{2+} ions and He. The calculations were performed with the optical potential and semiclassical methods. The relative collision energy concerned ranges from 0.1 meV to 10 keV and temperature from 10 K to 2×10^6 K. The

rate coefficients are compared with one available experimental value at 300 K and found to be in good agreement assuming that the measurement contains a significant amount of metastable contamination. The current results will be useful for numerical simulations of in low-temperature or ultracold plasmas, such as those produced in laboratories and a variety of astrophysical environments.

Acknowledgments

LBZ and PCS acknowledge support from NASA Grant No. NNG05GD98G and NSF Grant No. INT-0300708, JGW from China NSF Grant Nos. 10574018 and 10574020, RJB, JPG and HPL from the Deutsche Forschungsgemeinschaft grant Bu 450/7-3 and the Fonds der Chemischen Industrie, and MK from the Ministry of Education, Science, Sport, Culture and Technology, Japan Society for Promotion of Science (JSPS) for the US-JP Collaborative Research Program, and Collaborative Research Grant by National Institute for Fusion Science.

-
- [1] Flaks I P and Solov'ev E S 1958 *Sov. Phys. Tech. Phys.* **3** 577
 - [2] Kusakabe T, Nagai N, Hanaki H, Horiuchi T and Sakisaka M 1983 *J. Phys. Soc. Jpn.* **52** 4122
 - [3] Imai T W, Kimura M, Gu J P, Hirsch G, Buenker R J, Wang J G, Stancil P C and Pichl L 2003 *Phys. Rev. A* **68** 012716
 - [4] Zhao L B, Stancil P C, Gu J P, Liebermann H P, Funke P, Buenker R J and Kimura M *Phys. Rev. A* **71** 062713
 - [5] Kimura M, Dutta C M and Shimakura N 1994 *Astrophys. J.* **430** 435
 - [6] Stancil P C and Zygelman B 1996 *Astrophys. J.* **472** 102
 - [7] Zhao L B, Stancil P C, Gu J P, Liebermann H P, Li Y, Funke P, Buenker R J, Zygelman B, Kimura M and Dalgarno A 2004 *Astrophys. J.* **615** 1063
 - [8] Johnsen R and Biondi A 1978 *Phys. Rev. A* **18** 996
 - [9] Buenker R J and Peyerimhoff S D 1974 *Theor. Chim. Acta* **35** 33
 - [10] Buenker R J and Peyerimhoff S D 1975 *Theor. Chim. Acta* **39** 217
 - [11] Buenker R J and Peyerimhoff S D 1986 *Int. J. Quantum Chem.* **29** 435

- [12] Buenker R J 1982, *Current Aspects of Quantum Chemistry 1981: Studies in Physical and Theoretical Chemistry Vol.21* ed Carbo R (Elsevier, Amsterdam) p 17
- [13] Dunning T H Jr. 1989 *J. Chem. Phys.* **90** 1007
- [14] Roemelt J, Peyerimhoff S D and Buenker R J 1978 *Chem. Phys.* **34** 403
- [15] Mercier E, Chambaud G and Lévy B 1985 *Phys. Rev. A* **18** 3591
- [16] Ben-Itzhak I, Bouhnik J P, Chen Z, Esry B D, Gertner I, Heinemann C, Kock W, Lin C D and Rosner B 1997 *Phys. Rev. A* **56** 1268
- [17] Zygelman B and Dalgarno A 1988 *Phys. Rev. A* **38** 1877
- [18] Dalgarno A, Butler S E and Heil T G 1980 *Astron. Astrophys.* **89** 379
- [19] Butler S E and Dalgarno A 1980 *Astrophys. J.* **241** 838

TABLE I: Comparison of asymptotic separated-atom energies in eV between the present MRD-CI results and other calculations and experiments for the molecular states of NeHe^{2+} .

Asymptotic atomic state	Mol. state	This work	Theory ^a	Expt. ^b
$\text{Ne}^+(2s^22p^5\ ^2P^o) + \text{He}^+$	$1\ ^3\Sigma^+$	-16.259	-15.8	-16.383
	$1\ ^1\Sigma^+$	-16.250		—
	$1\ ^3\Pi$	-16.242		—
	$1\ ^1\Pi$	-16.242		—
$\text{Ne}^{2+}(2s^22p^4\ ^3P) + \text{He}$	$2\ ^3\Pi$	0.000	0.0	0.000
	$1\ ^3\Sigma^+$	0.009		
$\text{Ne}^{2+}(2s^22p^4\ ^1D) + \text{He}$	$2\ ^1\Sigma^+$	3.214	3.4	3.165
	$1\ ^1\Delta$	3.222		
	$2\ ^1\Pi$	3.226		
$\text{Ne}^{2+}(2s^22p^4\ ^1S) + \text{He}$	$3\ ^1\Sigma^+$	6.932	6.4	6.873

^a [15]

^b NIST Atomic Spectra Database (<http://physics.nist.gov/asd>.)

TABLE II: Comparison of dipole transition matrix elements between the MRD-CI results and other calculations for collisions of Ne^{2+} and He.

Mol. States		$ D_{ij} $ ($R = 2.5$ a.u.)			$ D_{ij} $ ($R = 8.0$ a.u.)		
i	j	This work	MCL ^a	BEN ^b	This work	MCL ^a	BEN ^b
3 $^1\Sigma^+$	1 $^1\Sigma^+$	0.667593	0.6852	0.7794	0.999923(-3) ^c	0.9(-3)	0.12(-2)
3 $^1\Sigma^+$	1 $^1\Pi$	0.399697(-1)	0.372(-1)	0.314(-1)	0.429621(-3)	0.2(-3)	0.2(-3)
2 $^1\Sigma^+$	1 $^1\Sigma^+$	0.619973	0.5825	0.4725	0.172508(-2)	0.5(-3)	0.24(-2)
2 $^1\Sigma^+$	1 $^1\Pi$	0.307561(-1)	0.351(-1)	0.259(-1)	0.227581(-3)	0.1(-3)	0.1(-3)
1 $^1\Delta$	1 $^1\Pi$	0.200397(-1)	0.170(-1)	0.103(-1)	0.399983(-3)	0.3(-3)	0.2(-3)
2 $^1\Pi$	1 $^1\Pi$	0.715660	0.7182	0.7601	0.150128(-2)	0.4(-3)	0.18(-2)
2 $^1\Pi$	1 $^1\Sigma^+$	0.140005(-1)	0.53(-2)	0.13(-2)	0.351426(-3)	0.3(-3)	0.2(-3)
2 $^3\Pi$	1 $^3\Pi$	0.872135	0.8821	0.9181	0.197682(-2)	0.9(-3)	0.29(-2)
2 $^3\Pi$	1 $^3\Sigma^+$	0.181950(-1)	0.182(-1)	0.110(-1)	0.586824(-3)	0.3(-3)	0.2(-3)
1 $^3\Sigma^-$	1 $^3\Pi$	0.129002(-1)	0.76(-2)	0.7(-3)	0.566041(-3)	0.3(-3)	0.2(-3)

^a[15]

^b[16]

^c $A(-B) = A \times 10^{-B}$

TABLE III: Fitting parameters of rate coefficients for radiative charge transfer from $\text{Ne}^{2+}(^1\text{S}, ^1\text{D}, ^3\text{P}) + \text{He}$ to $\text{Ne}^+(^2\text{P}^o) + \text{He}^+$. a_i and c_i are in units of $\text{cm}^3 \text{s}^{-1}$ and K, respectively.

Param.	$\text{Ne}^{2+}(^1\text{S})$	$\text{Ne}^{2+}(^1\text{D})$	$\text{Ne}^{2+}(^3\text{P})$
a_1	2.2369469(-14) ^a	1.3211271(-14)	3.9098970(-15)
b_1	1.0267012(-01)	6.1739477(-02)	1.1436961(-01)
c_1	6.6197182(+07)	-1.2291226(+07)	-1.6304181(+07)
a_2	-2.0882541(-14)	-1.1220290(-14)	-3.2168262(-15)
b_2	2.2212160(-01)	1.3581148(-01)	2.7272387(-01)
c_2	4.2729689(+04)	9.7408175(+04)	6.2875500(+04)

^a $A(-B) = A \times 10^{-B}$

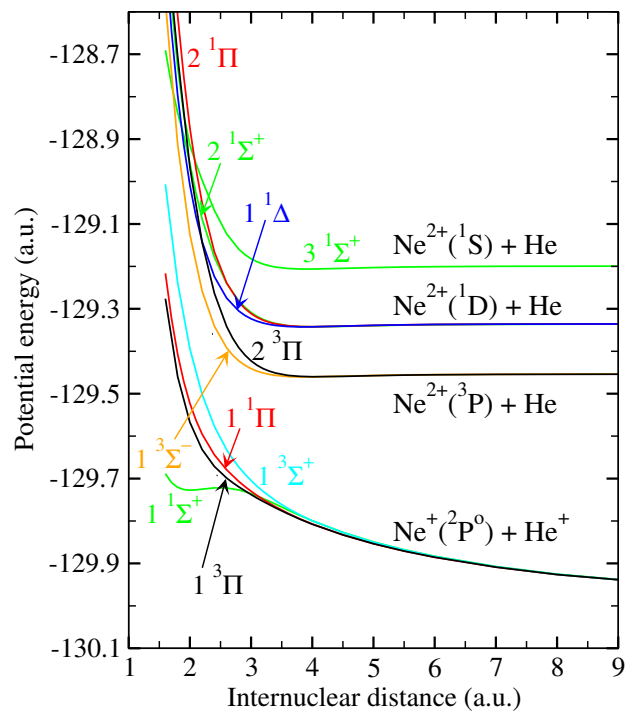


FIG. 1: The adiabatic potentials of the NeHe^{2+} system.

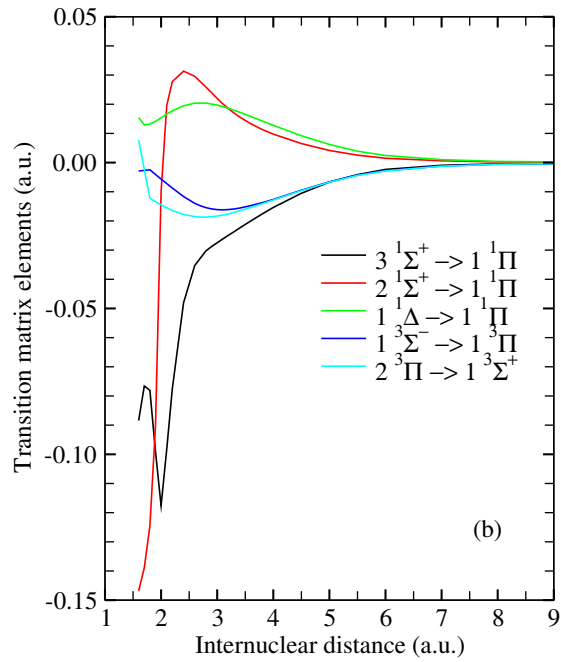
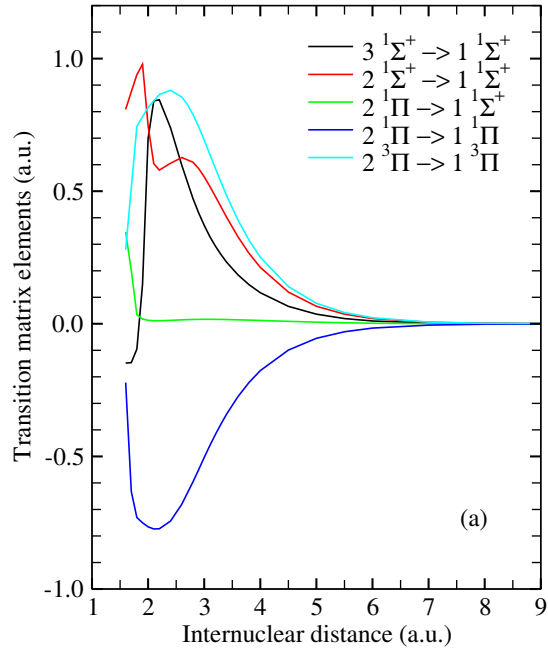


FIG. 2: The dipole transition moments for radiative decay from $\text{Ne}^{2+} ({}^1\text{S}, {}^1\text{D}, {}^3\text{P}) + \text{He}$ to $\text{Ne}^+ ({}^2\text{P}^o) + \text{He}^+$.

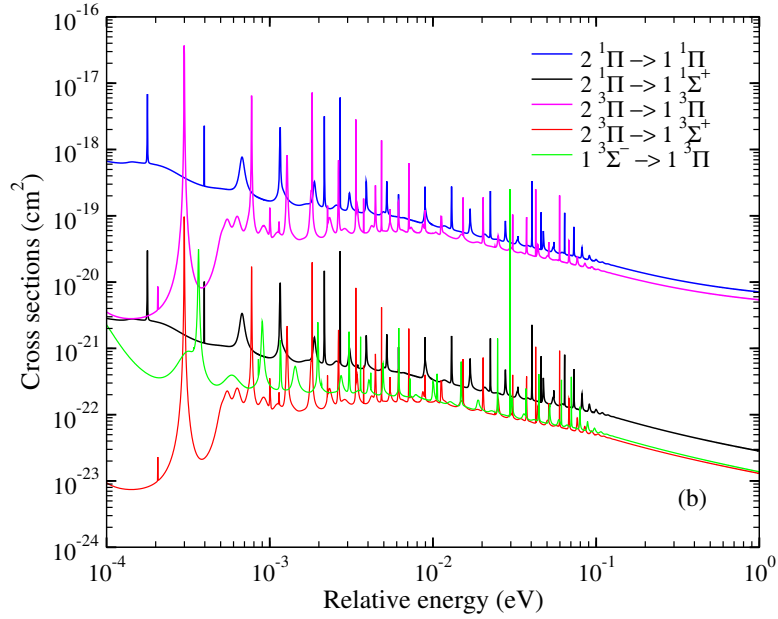
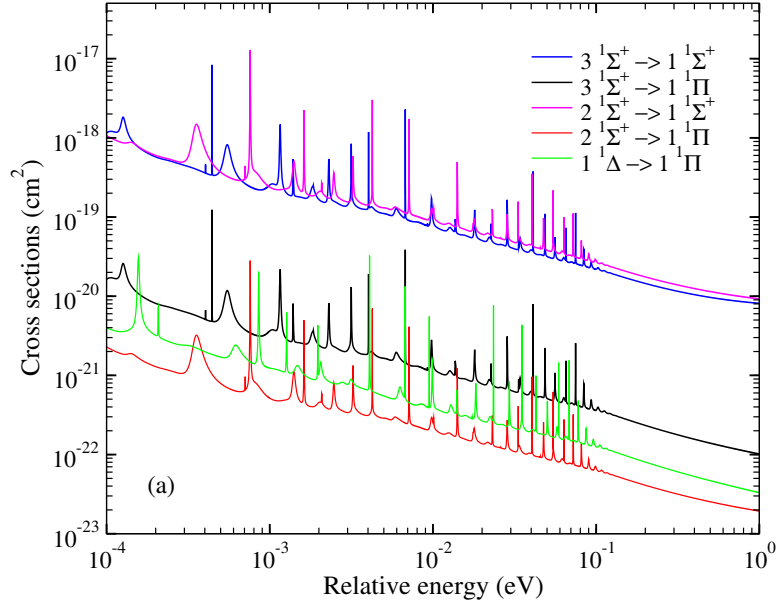


FIG. 3: State-to-state cross sections for radiative charge transfer as a function of collision energy. All the curves are calculated with the optical potential method in equation (5). The cross sections are not multiplied by the approach probability factor p_{AS} .

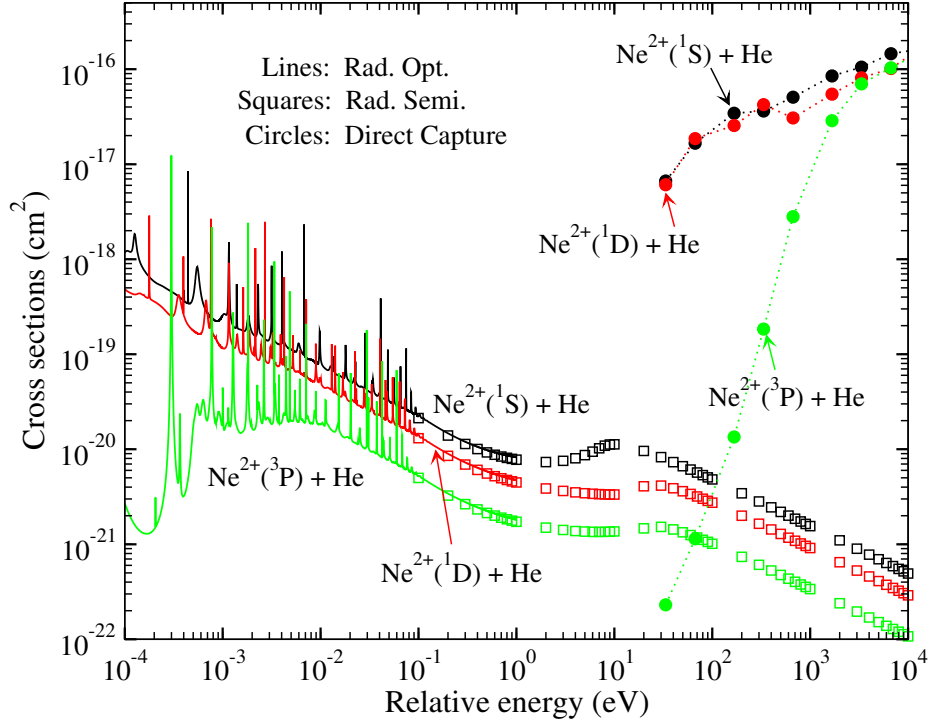


FIG. 4: Total cross sections for radiative charge transfer to $\text{Ne}^+(^2\text{P}^o) + \text{He}^+$ from (1) $\text{Ne}^{2+}(^1\text{S}) + \text{He}$, (2) $\text{Ne}^{2+}(^1\text{D}) + \text{He}$ and (3) $\text{Ne}^{2+}(^3\text{P}) + \text{He}$, respectively. Radiative charge transfer cross sections are obtained with the optical potential method (*curves*) and with the semiclassical method (*open squares*), and direct charge transfer cross sections are from Imai *et al* [3] (*filled circles*).

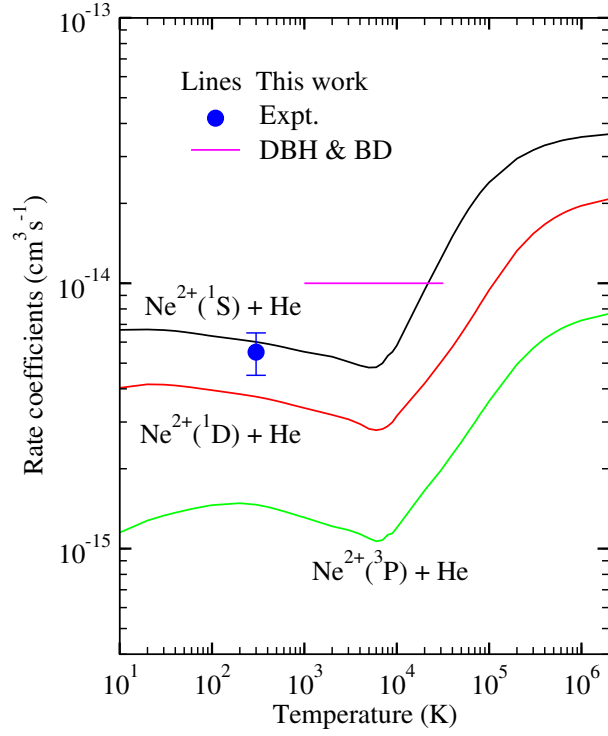


FIG. 5: Comparison of the current rate coefficients (*solid lines*) and experiment (*filled circle*) for radiative charge transfer to $\text{Ne}^+(^2P^o) + \text{He}^+$ from (1) $\text{Ne}^{2+}(^1S) + \text{He}$, (2) $\text{Ne}^{2+}(^1D) + \text{He}$ and (3) $\text{Ne}^{2+}(^3P) + \text{He}$. The estimate of Dalgarno, Butler and Heil [18] and Butler and Dalgarno [19] is given (DBH & BD).